Measurements of droplet size in a two-phase mixing layer using an optical probe with new shape design

S. Marty*[1], J.P Matas [1], A. Cartellier [1], S. Gluck [2]
[1]LEGI CNRS/Grenoble University Grenoble, France
[2] A2 Photonic Sensors, Grenoble, France
sylvain.marty@legi.grenoble-inp.fr, jean-philippe.matas@legi.grenoble-inp.fr,
alain.cartellier@legi.grenoble-inp.fr and sgluck@a2photonicsensors.com

Abstract

Most current turboreactors or rocket engines use gas assisted atomization to produce a fuel spray. Atomization is carried out by the destabilization of a slow liquid film, sheet or jet of fuel by a fast gas stream. To optimize such engines, the mechanisms leading to droplets formation need to be precisely understood. Among these, the stripping mechanism has been thoroughly investigated and phenomenological models providing some drop characteristics are already available. Yet, these proposals have been tested over a limited range of flow conditions and our objective is to check their validity over a wider range of liquid and gas flow velocities. In that perspective, new optical probes with short ($10\ \mu m$) sensing lengths have been manufactured. We discuss their performances in terms of drop size, velocity and flux measurements in comparison with former versions of such sensors whose sensing lengths was at least twice longer. The new sensor is then used in a two-phase mixing layer. Chord distributions as well as the Sauter mean diameters are presented for gas velocities between 20 m/s and 90 m/s and for dynamic pressure ratios M from to 2 and 16. The analysis of these results indicates that the mean drop size primarily depends on the gas velocity. Also, chord distributions normalized by the mean value are weakly modified when changing M. These features indicate that the destabilizing mechanisms are quite similar over the considered range of flow conditions.

Introduction: spray characteristics in a two-phase flow injector

Most of current turboreactors or rocket engines use gas assisted atomization to produce a fuel spray. Atomization is carried out with the destabilization of a slow liquid film, sheet or jet of fuel by a fast gas stream. The characteristics of the produced spray are essential for the quality of combustion. For example a low Sauter diameter of droplets decreases the amount of pollutants emitted by a turboengine. To improve the efficiency of such engines we need a good understanding of the atomization mechanisms. These mechanisms can be partly controlled through the design of injectors (recess length, diameter of fuel channel, nozzle thickness and many others geometrical considerations) or by choosing optimal fuel and air mass flow conditions. A good review of the different techniques for atomization can be found in [1]. Previous investigations on droplets stripped off the interface

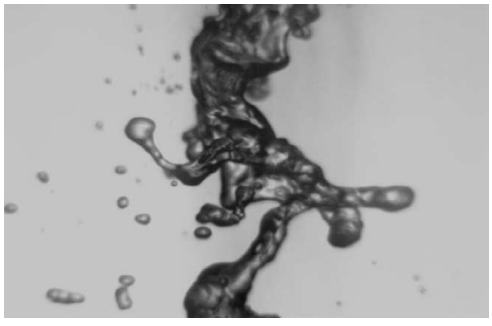

Figure 1. An example of atomized slow liquid flow by a rapid air stream

(Figure 1) have shown that atomization is driven by three successive instabilities. First, longitudinal waves are formed by a Kelvin-Helmholtz type instability whose most amplified wavelength is controlled by the gas vorticity thickness δ_G at the injector exit (Villermaux & Marmottant 2004 [2]). The axial frequency prediction was recently

*Corresponding author: sylvain.marty@legi.grenoble-inp.fr

improved by accounting for the presence of the splitter plate between gas and liquid (Matas et al. 2011 [3]). Second, ligaments arise on the wave crests due to a wind induced Rayleigh-Taylor instability (Hong et al. 2002 [4], Varga et al. 2003 [5]). These ligaments then break into droplets (Villermaux 2007 [6]). A phenomenological model has been proposed for the mean drop size D (Hong et al. 2002 [4]): D varies as $\delta_G\ W_e^{-1/2}$ where the relevant Weber number We is defined as $We = (\rho_G(U_G - U_C)^2\delta_G)/\sigma$, U_C being the convective velocity of the axial instability. This proposal proved valid both for planar and axisymmetric configurations (Ben Rayana et al. 2006 [7]). Yet this model was only tested in the limit of large dynamic pressure ratios $M = (\rho_G U_G^2)/(\rho_L U_L^2)$, namely for M about 10 and above, corresponding to conditions encountered in cryotechnic engines and in turboreactors during take off. The study of Matas et al. [3] showed that the dimensionless K-H instability frequency $f\delta_G/U_G$ is also controlled by M, for M values down to unity or below. These low M values correspond to injection during cruise and re-ignition. In this paper, our objective is to test whether the mean drop size is affected when M varies. To access drop size and flux we use a single conical optical probe. This technique was proposed and validated by Cartellier [8] for bubble detection. Cartellier & al. 2004 [10] and Hong & al. 2004 [11] exploited such probes for droplet detection and they showed that droplet size statistics are weakly sensitive to signal processing parameters. These authors argue that a reduction of the probe sensitive length should lead to a better detection of small inclusions (say below $10 - 15\ \mu m$) and will thus improve the measuring capabilities of these sensors. Recently, Saito & al. [12] developed a similar technique using a truncated optic fiber with a special design. Thanks to micro manufacturing techniques, the A2PS company recently succeeded in producing probes with a significantly smaller sensing length. The question was therefore to check the performances of these new sensors.
In the first part of this paper, after a quick summary of the principles of optical probe measurements, we discuss the capability of the new probes with respect to the detection of very small droplets. In the second part, this sensor is used on a planar two-phase mixing layer and we analyze the dependency of the spray characteristics on M.

Optical probe qualification

Optical probe measure technical

Optical probes are a weakly intrusive sensor giving access to drop characteristics. In particular, their output consists in the joint product density of velocities and chords. These sensors can be operated in dense sprays (even if they are optically thick), as well as on drop with distorted shapes. Their functioning, explained in [8], is briefly summarized here after.
The probe consists of an optical fiber whose extremity has been shaped into a cone. The light sent through the fiber is reflected at its tip. As the light intensity traveling back through the fiber varies with the refractive index of the phase enclosing its very tip, such sensors detect the passage of droplets. A Typical signal gathered in a spray is shown in figure 2. In this example, the gas phase corresponds to the upper level voltage V_Gref while the smallest amplitude V_Lref corresponds to a probe tip fully immersed in water. Here V_Gref is about 4.5 volts, while V_Lref is about 1.5 volt. Every drop in the signal corresponds to a droplet hitting the probe. For each inclusion, a signal processing program (SOG6 property of A2PhotonicSensor) determines a set of characteristic events $p1$ to $p6$. The residence time of the probe in the drop T_L is defined as the duration between $p1$ and $p3$ events. The dewetting

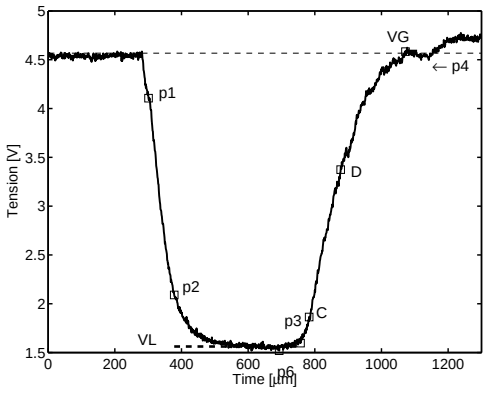

Figure 2. Example of a raw signal recorded when a droplet hits the probe

process starts at the event $p3$ and is achieved at $p4$. The dewetting time T_M is defined between two selected points C and D defined by their amplitude with respect to the full signal dynamics: typical thresholds are 10% for C and 60 or 80% for D. We know that, under some conditions, T_M is proportional to the local interface velocity. More

precisely, this duration is given by the sensitive length Ls of the probe divided by the interface velocity. The corresponding chord for each drop hit by the probe is then deduced from $C = Ls.T_L/T_M$. More detailed explanations on the signal processing can be found in Hong & al. 2004 [11].
The output of the signal processing consists in the joint product density of velocities and chords. From this, one can deduce a number of variables [9] including concentration, number density fluxes and various distributions. Yet the determination of the size distribution is generally delicate and requires some assumptions. For example, for spherical inclusions, Clark et Turton [13] provided the relation between chord $P(C)$ and diameter $P(R)$ distributions:

$$P(C) = \int_{C/2}^{R_{max}} \frac{C}{2R^2} P_d(R) dR \text{ and } P(R) = \frac{P_d(R)}{R^2} \left(\int \frac{P_d(R)}{R^2} dR \right)^{-1} \quad (1)$$

where $P_d(R)$ is the detected diameter distribution. Various inversion procedures have been proposed to exploit equation 1, but they all suffer from various drawbacks that lead to uncertainties difficult to control. In the present investigation, we prefered a more direct approach. Indeed, Liu 1995 [14] has shown that the mean Sauter diameter D_{32} can be directly deduced from the mean chord using $D_{32} = 3/2 \times C_{10}$,valid for spherical and ellipsoidal inclusions. With this method, we merely have to ensure a correct convergence of the chord distribution [15].

Optimized probe sensing tip

Different kinds of optical sensing tips have been developed, based on the assumption that the lower Ls, the better the detection of small droplets. Standard conical probes exploit optical fibers with a core diameter about $100\ \mu m$ and their sensing length is typically about $40 - 50\ \mu m$. In order to concentrate most of the incoming light in the center of the fiber, we exploited fibers of lower core diameters and, in addition, we designed specific shapes to obtain thinner physical tips. As a result, figure 3, the new optimized sensing tip has a sensing length reduced

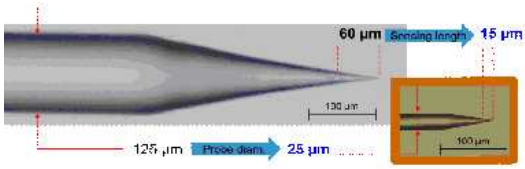

Figure 3. Standard and new optical probes with a smaller sensitive length

by a factor about 4 compared with standard sensors. In addition, their reduced overall physical dimensions make these new probes much less intrusive.

Test of the new probe

The new probe was tested by way of a comparison with a standard conical probe of longer sensing length in the same flow conditions. A dedicated set-up was designed that produces an almost spatially uniform spray in an horizontal tube. The air flow is produced by a compressor - its temperature is controlled by a thermal exchanger - goes through a honey comb and then flows in an horizontal tube of diameter $\phi = 120\ mm$. High pressure injectors ($80\ bars$) with $\phi\ 30\ \mu m$ holes located at the tube entrance produce fine droplets. In this set-up, the maximum air velocity is $U_G = 18\ m.s^{-1}$. The liquid flow is controlled by selecting the number of active injectors. The water flow rate Ql is about $2.0\ g.s^{-1}$ when using two injectors, and $5.0\ g.s^{-1}$ with four injectors. Measurements were taken $0.8\ m$ downstream the injectors and on the tube axis. Four conditions were considered, by varying the air velocity ($12\ m.s^{-1}$ and $18\ m.s^{-1}$), and by changing the number of active injectors (2 and 4). Typical signals delivered by the two probes are exemplified in figure 4(a) and 4(b). The falls in the signal due to droplets hitting the probe are clearly perceived. The reference liquid level V_L is taken as the minimum amplitude: the latter is quite stable in time. However, in both cases, the signals experience strong variations of the gas voltage. This behavior is most probably related with the dewetting dynamics, as the dewetting is usually not completed before the next drop hits the probe. The relatively low gas velocities used in this test probably make this problem worse. First, measurements were taken with a standard conical probe whose sensitive length - defined between 10% and 60% thresholds - is about $18\ \mu m$. These data will be considered as the reference in the following discussion. Table 1 provides some average quantities for the four flow conditions.
These results are consistent. In particular, the mean droplet velocities recorded by the probe are about 30% below the gas velocity. This is expected because the short length of the tube does not provide a long enough transit time for droplets to reach the gas velocity in the horizontal direction. Mean chords are very close whatever the flow

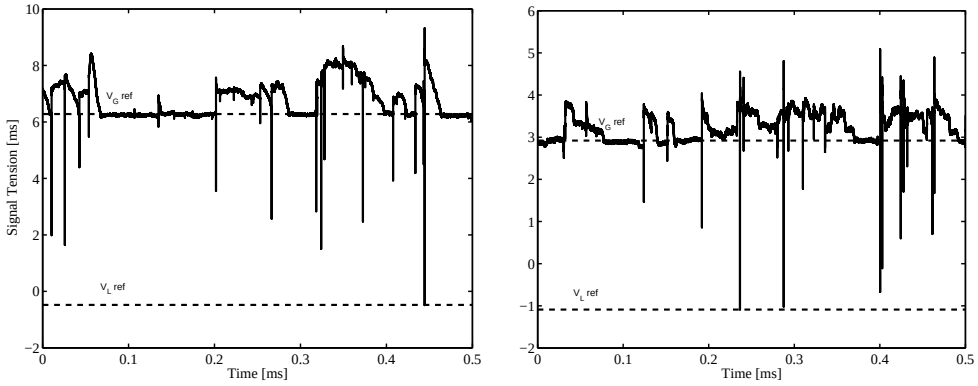

(a) $Ls = 18\mu m$ (b) $Ls = 10.9\mu m$

Figure 4. Raw signals from the two probes at $Ug = 18\ m.s^{-1}$ and for the largest liquid flow rate

Optical Probe				
Injector	2	2	4	4
$U_G\ m.s^{-1}$	12	18	12	18
$< V >\ m.s^{-1}$	9.6	12.6	8.8	12.2
$C_{10}\ \mu m$	12.2	11.6	14.9	12.2
$J_L\ m.s^{-1}.10^{-4}$	2.4	2.30	5.3	4.9

Table 1. Some average quantities as measures by the experience with classical $1C$ probe with $Ls = 18\ \mu m$

condition, with a maximum relative deviation about 22%. Again this is expected as the injectors operate in the same regime for all experimental conditions. Last the measured fluxes are nearly multiplied by two when doubling the liquid flow rate. Now, let us consider the same measurements achieved with the new probe. The corresponding signal, shown figure 4(b) are quite similar to those from the $1C$ probe with a slightly lower dynamic $V_G - V_L$. The results are given in table 2. Mean velocities, mean chords and local fluxes are quite similar, with a typical difference between probes about 20%. The largest difference, about 30%, is observed for the mean chords at the higher flow rate. This is not too bad according to the raw signal quality. We already mentioned the strong fluctuations of the gas level which complicate signal processing. The presence of overshoots - apparently more frequent on thin probes - introduced an extra complexity which was not considered in the present version of the signal processing. The comparison of chord distributions, figure 5(a) and 5(b), exhibits interesting features. On these distributions, the minimum bin interval is about $2\ \mu m$: such a small value was selected to better compare the probe capabilities. Let us consider the chords below $20\ \mu m$. Clearly, the finest probe detects a larger population in the first bin compared with the larger one, while others bins are not affected (see inserts). Although smaller droplets or chords cut through droplets are better detected by the thinnest probe, the shape of the chord pdf, and in particular the position of its maximum, is nearly the same for the two probes. Strong differences in the pdfs were found when the sensing length was reduced from $60\ \mu m$ to about $20\ \mu m$ (see reference [10]). Here, a reduction from $18\ \mu m$ to $10\ \mu m$ only marginally alters the pdf. Thus, at least for the spray considered, a further diminution in the probe size will probably not lead to any significant gain.

Application to the investigation in an air-water mixing layer

The new probes with a smaller sensitive length have been used to characterize the spray produced by a planar air-water mixing layer. The experiment, figure 6(a), is a modified version of the bench previously used by Raynal (1997) [16] and later by Hong (2003) [17], Ben Rayana (2007) [18]. This injector is composed of two parallel channels: the upper channel corresponds to the gas stream with a maximum mean gas velocity about $100\ m.s^{-1}$.

L_S	18	10.9	18	10.9
Injector	4 injectors		2 injectors	
$< V > \ m.s^{-1}$	12.2	15.3	12.6	12.8
$C_{10}\ \mu m$	12.2	17.1	11.6	12.9
$J_L\ m.s^{-1}.10^{-4}$	4.9	4.1	2.3	1.7

Table 2. Comparison between $1C$ and $1C3C$ probes measurements at $U_G = 18\ m.s^{-1}$ for $Ql\ =\ 2.0\ g.s^{-1}$ and $5.0\ g.s^{-1}$

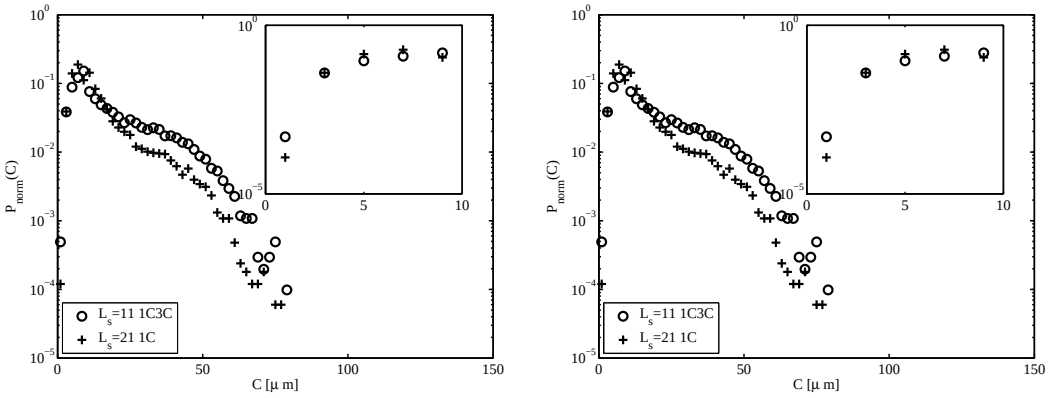

(a) Q_l max. (b) Q_l min.

Figure 5. Distribution of chords for two probes: $\circ\ =\ 1C3C$ and $+\ =\ 1C$ at $U_G = 18\ m.s^{-1}$

The lower channel is fed with water, which stands in lieu of fuel. In order to damp velocity perturbations, honey

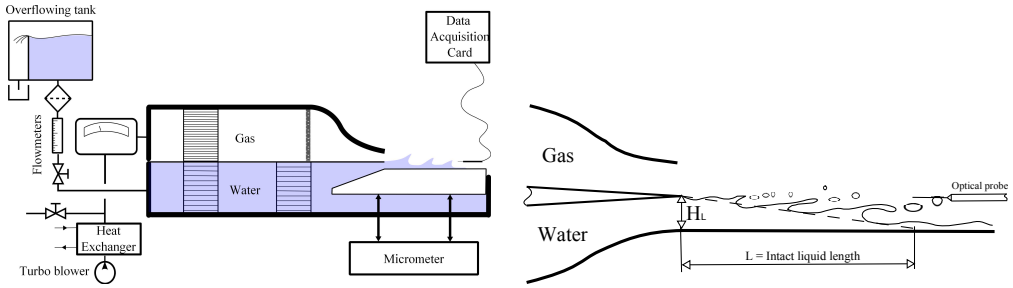

(a) Illustration of the planar injector geometry and relative position of the optical probe (b) Relative position of the probe in the spray

Figure 6. The planar injector

combs are inserted in each channel, with an additional porous plate for the gas. Both channels end with smooth convergent profiles with a high contraction ratio (above 10). The two main parameters controlling the injection are the mean gas velocity U_G and the mean liquid velocity U_L. Our objective here is to investigate the influence of injection conditions in terms of the dynamic pressure ratio M on the average size of drops obtained from primary atomization.

To this aim, the experiment has been adapted in order to vary the thickness H_L of liquid layer at the nozzle of the injector from $10\ mm$ down to about $1\ mm$. Thanks to this modification, the mean liquid velocity can be significantly increased and much lower dynamic pressure ratios M can be obtained. The results have been gathered for a fixed injector geometry with a water thickness at exit $H_L\ =\ 6\ mm$, and a gas thickness $H_G\ =\ 10\ mm$.

Hong (2004) [11] carried out optical probe measurement in a similar configuration, and he has shown that spatial variations of the drop characteristics (size, flux) are quite strong. Therefore, care was taken, when varying M, to collect data at the same relative position (figure 6(b)). Along the vertical axis the probe is aligned with the splitter plate, while its downstream position is located at the end of the theoretical liquid intact length L. The latter has been shown (Raynal 1997 [16]) to vary as:$L/2H_L \approx 6/\sqrt{M}$ for M less than about 30. At such a position, no more water can be stripped off by the air flow and therefore we can consider that primary atomization is completed. With these considerations concerning the position, droplet chord distributions were collected for M varying from 16 to 2, with U_G varying between 20 to 90 $m.s^{-1}$, and U_L between 0.1 to 1 $m.s^{-1}$. The probe used for these measurements is the probe with a sensitive length - defined between the thresholds 10% and 60% of the maximal signal dynamics - equal to 10 μm. To ensure the stability of conditions, each series with M fixed does not exceed a 10 min acquisition. This duration is sufficient to ensure a correct convergence of the measurements (see reference [15]). The probe is cleaned with isopropanol before each series. Processing and post-processing parameters were the same as in previous studies [4] and [10], in particular the cut-off value for large drop sizes is fixed at 2%. This means that 2% of the largest chords are eliminated: the later correspond indeed to very rare events such as large waves or non broken ligaments that may occasionally be detected at the selected measuring position. Graph 7 shows D_{32} values deduced from the average chord C_{10}, as a function of the gas speed. As said in the introduction, wave crests turn into ligaments under the action of a Rayleigh-Taylor instability: this implies a dependency of D_{32} upon the Weber number. In our case, this dependency turns into $D_{32} \approx U_G^{-5/4}$ if we use a simplified but adequate approach of the Kelvin-Helmholtz primary instability [4]. A continuous line is drawn to visualize the expected $-5/4$ slope. The three following series $\circ$, $\square$ and $\lozenge$ are respectively for $M = 16$, $M = 8$ and $M = 4$. The last series , symbol $\bullet$, is for $M = 2$. For $U_G = 30m.s^{-}1$, the Sauter mean diameter is large, about

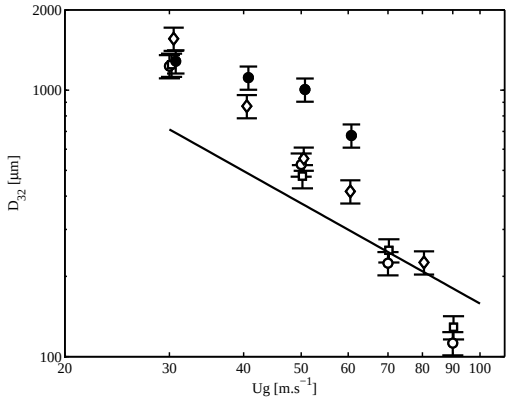

Figure 7. Mean Sauter diameter of droplet D_{32} as a function of gas velocity U_G in series of M: $\circ$ $M = 16$; $\square$ $M = 8$; $\lozenge$ $M = 4$ and $\bullet$ $M = 2$

1600 μm. Its value drops down to 115 μm for the highest gas velocity considered, namelly $U_G = 90\ m.s^{-}1$. As expected, we observe a strong decrease of D_{32} with the gas velocity. The important conclusion here is that the Sauter mean diameter is almost insensitive to M in the range $M = 4$ to $M = 16$. The maximum deviation at a given gas velocity is 21%. In other words, D_{32} is nearly insensitive to liquid velocity. This indicates that the interfacial instabilities governing drop size remain the same over this range of parameters: we will go back to this feature when discussing chord size distributions. Deviations from the above mentioned trend happen in two cases. For $M = 2$, the mean drop size is slighly larger than for others series at fixed M. In addition, data collected at $U_G = 20m.s^{-}1$ (not shown in the figure) provides much larger D_{32}. When examining the raw signals at such small gas velocity, periodic signatures are clearly visible: these are the marks of the passage of axial waves at the reference point. Similar features happen in the $M = 2$ series although they are not so well distinguishable. In previous experiments achieved for $M = 16$ and $H_L = 10\ mm$, such motif were not detected at the selected position, but they were observed when moving the probe closer to the interface. In the present experiment, it is therefore likely that the probe is much closer to the interface than initially believed. A possible explanation to that could be related with the change in H_L which is here 6 mm. We do not expect a change in the liquid intact length (the latter should follow the expected law $L/2H_L \approx 6/\sqrt{M}$). Instead, it is likely that the liquid film running on the bottom wall becomes thick enough to interact with the probe (visualization indicates that the interface of this film fluctuates significantly). This is supported by the fact that such defects are mainly observed at low gas velocities i.e. when the flux of drops stripped off the liquid incoming stream is the weakest so that most of the

liquid flow rate goes within the film. Similarly, low M values correspond to large liquid velocities and thus to larger flow rates in that film. Going back to the data gathered at larger M, a continuous line is drawn in 7 to visualize the expected $-5/4$ slope. The data are close to the expected $-5/4$ slope but the latter is not quite recovered in the present conditions while the agreement was very good in the experiments performed at $M = 16$ and $H_L = 10\,mm$ (Ben Rayana Iclass 2006 [7]). It is thus possible that the instable liquid film remaining on the bottom wall also affects in some way the measured chord distributions in most of the experimental conditions. Another argument in that direction is that the mean chords are neatly larger here compared with those previously measured [7]. The influence of the bottom liquid film was unexpected. Clearly a new set of data needs to be collected at a higher height to test whether the present measuring campaign was affected by the film or not, and to what extent. Yet, the weak dependence of D_{32} on the liquid velocity is encouraging. Another way to check this trend is to examine the chord distributions. Figure 8(a) and 8(b) show the probability density function of the dimensionless chord C/C_{10} - where C_{10} is the chord arithmetic mean - for two cases. These distributions are well converged with a minimum of 20000 droplets per record. Such a number of events allow us to set the class width at its minimum, namely half the probe sensitive length. Figure 8(a) provides five chord distributions for different U_G and at a constant M, while in figure 8(b) U_G is fixed and M is varied. With the new probe, the pdf happens to be better resolved especially

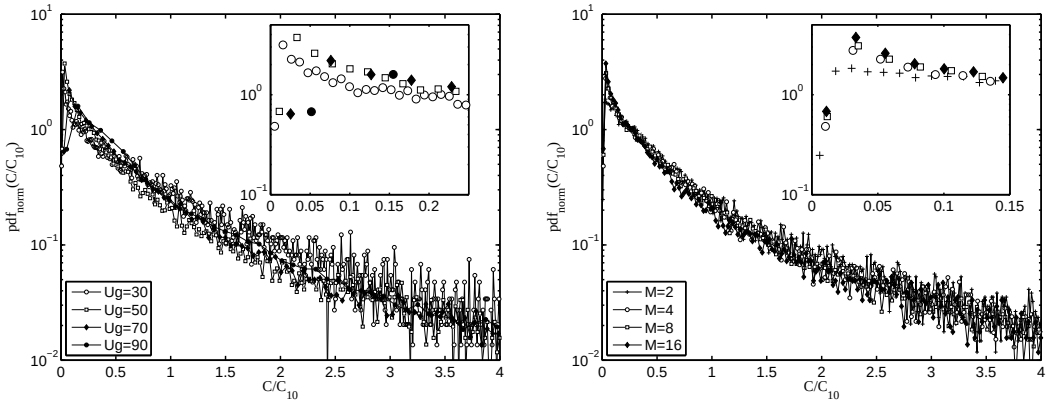

(a) $M = 16$ (b) $U_g = 50 m.s^{-1}$

Figure 8. Dimensionless mean chord C/C_{10} probability density functions at $M = 16$ for different gas velocities (left) and for at $U_g = 50\ m.s^{-1}$ for different M (right). Inserts: pdf behaviour in the limit of small C/C_{10}

in the low chord limit. In particular, the pdf maximum is now detected (see inserts figure 8(a) and 8(b)) while it was not systematically so when using probes with a longer sensing length. Note that although the resolution on dimensional chord measurements is the same for all conditions, the classes used to plot the pdf are not identical in terms of C/C_{10}. This is why only a few data are available in the inserts when the C_{10} is large (i.e. low U_g). In addition, that class width affects the dispersion observed at large C/C_{10} that correspond to rare events. For all the flow conditions considered, the pdfs happen to be almost identical, indicating that the break-up process are indeed similar. These pdf are clearly controlled, at first order, by the mean chord size, a feature consistent with the findings of Marmottant and Villermaux 2004 [2] on axi-symmetrical injectors and for U_g up to $50\ m.s^{-1}$. Further analysis is required to test whether the gamma law behavior identified by these authors can be recovered from the distributions measured with optical probes.

Conclusion

The detailed analysis of sprays require reliable measurements of drop characteristics, including size, velocity and flux. Optical probes have already been used for such measurements (see Hong & all 2004 [11]). Yet, in their standard version, their sensing length was never less than $Ls = 18\ \mu m$ so that the detection of small chords (say below about $5 - 10\ \mu m$) that correspond either to small droplets or to chords cut through larger drops, was subject to a bias whose magnitude was unknown ([10]). New optical probes have been produced whose sensing length ($Ls = 10.9\ \mu m$) is nearly half the standard value. We tested their measuring capability on a dedicated test bench producing a spatially homogeneous spray of water drops in an air stream above $10\ m.s^{-1}$. The comparison of the chord distributions show that the thinner probe indeed detects many more events in the first bin (range $2\ \mu m$). Otherwise, the chord distributions remain nearly identical for chords above about $5\ \mu m$. This indicates that the technique is indeed reliable down to such small dimensions (although that result does not imply that drop sizes

down to such values are correctly detected). Mean chords, mean velocities and fluxes detected by the standard probe and by the thinner probe typically agree within 20% or less.
We then exploited the new probe on a planar air water mixing layer. The objective was to check the influence of the dynamic pressure ratio M on drop size. Measurements indicate a weak sensitivity of the mean drop size and of the chord distributions on M in the range 4 to 16. Some deviations were however observed for $M = 2$ and also at the smallest air velocity $U_G = 20\ m.s^{-1}$. As the height of the liquid exit has been diminished down to $6\ mm$, it is likely that the probe detected not only the drops but also the waves at the surface of the liquid film formed on pre-filming zone. Despite this unexpected difficulty, the weak sensitivity of drop size to M indicates that the mechanisms of drop formation remain similar in the conditions considered. This investigation has to be repeated for another probe position in order to confirm this trend. An encouraging aspect is that all the chord distributions measured with the thinner probe exhibit a clear maximum, who was not always seen when using standard probe. Such a feature will greatly ease the comparison with modelling proposals in particular regarding the shape of the size pdfs. Further investigations will be devoted to the analysis of the fluxes as these are important quantities for applications and for the implementation of initial conditions in numerical simulations.

Acknowledgment: The research leading to these results has received funding from the European Union Seventh Framework Programme ($FP7/2007-2013$) under grant agreement $n^{\circ}265848$ and was conducted within the **FIRST** project.

References

[1] Lightfoot M.,"Fundamental classification of atomization processes", Atomization and Sprays,19(11):1065-1104,2009.
[2] Marmottant P., and Villermaux E.,"On spray formation", J. Fluid Mech., 498 (2004), 73-111.
[3] Matas J.-Ph., Marty S., Cartellier A., "Experimental and analytical study of the shear instability of a gas-liquid mixing layer", Phys. Fluids 23, 094112 (2011); doi:10.1063/1.3642640.
[4] Hong M., Cartellier A. and Hopfinger E. J.,"Atomization and mixing in coaxial injection" (2002), Proc. 4th Int. Conf. On Launcher Technology. Liege, Belgium (3- 6 Dec. 2002).
[5] Varga C. M., Lasheras J. C., and Hopfinger E. J.,"Initial breakup of a small-diameter liquid jet by a high-speed gas stream", J. Fluid Mech., 497 (2003), 405-434.
[6] Villermaux E., "Fragmentation", Ann. Rev. Fluid Mech., (2007) 39:419-46
[7] Ben Rayana F., Cartellier A., Hopfinger E.," Assisted atomization of a liquid layer: investigation of the parameters affecting the mean drop size prediction", (paper ICLASS06-190), CD Proc. ICLASS 2006, Aug. 27 - Sept. 1, Kyoto, Japan, ISBN 4-9902774-1-4, Publ. Academic Publication and Printings Co., 2006.
[8] Cartellier A.,"Simultaneous void fraction measurment, bubble velocity, and size estimate using a single optical probe in gas-liquid two-phase flows", Rev. Sci. Instrum., vol. 63, pp5442-5453, 1992.
[9] A. Cartellier,"Post-treatment for phase detection probes in non uniform two-phase flows",Int. J. Multiphase Flow.,Vol. 25, 201-228, 1999
[10] Cartellier A., Ben Rayana F.,"Dispersed phase measurements in sprays using optical probes", 3rd int. Symp. on Two phase flow modeling and Experimentation, Pisa, 22-24 sept. 2004
[11] M.Hong, A. Cartellier, E. Hopfinger,"Characterization of phase detection optical probes for the measurement of the dispersed phase parameter in sprays", International Journal of multiphase flow,vol. 30, 615-648, 2004
[12] T. Saito,K. Matsuda,Y. Ozawa,S. Oishi and S. Aoshima."Measurement of tiny droplets using a newly developed optical fibre probe micro-fabricated by a femtosecond pulse laser" Measure. Sci. Tech. 20 114,002, 2009
[13] Clark N.N., Turton R.,"Chord length distributions related to bubble size distributions in multiphase flows",Int. J. Multiphase Flow 14, 413-424, 1988.
[14] W.Liu and N.N. Clark, "Relationships between distributions of chord lengths and distributions of bubble sizes including their statistical parameter", Int. J. Multiphase Flow., 21 6, 1073-1089 (1995).
[15] S. Marty, J.P Matas, A. Cartellier, "Study of a liquid-gas mixing layer: Shear instability and size of produced drops", 3rd INCA symposium, 17-18 november 2011, Toulouse
[16] L. Raynal, "Instabilité et entrainement à l'interface d'une couche de mélange liquide-gaz", Thèse UJF (1997).
[17] M. Hong, "Atomisation et mélange dans les jets coaxiaux Liquide-gaz", Thèse INPG, LEGI (2003).
[18] F. Ben Rayana, "Contribution à l'étude des instabilités interfaciales liquide-gaz en atomisation assistée et tailles de gouttes", Thèse INPG, LEGI (2007).